

ANALYSIS OF THE DEFICIENT LENGTH PREDICTION ERROR METHOD IN A HEARING AID'S FEEDBACK CANCELLER

Victor Bissoli Nicolau and Márcio Holsbach Costa

Departamento de Engenharia Elétrica, Universidade Federal de Santa Catarina
Centro Tecnológico, Cidade Universitária, 88040-900, Florianópolis-SC, Brazil
phone: + (55) 48 3721-9506, fax: + (55) 48 3721-9280, email: victor@lpds.ufsc.br, costa@eel.ufsc.br

ABSTRACT

This work presents a statistical analysis of the deficient length Least Mean Square algorithm combined with the prediction error method applied to feedback cancellation in hearing aids. Deterministic recursive equations to the mean coefficient behaviour of the adaptive filters were derived in order to assess the performance of the algorithm. The expected theoretical behaviour was compared with Monte Carlo simulations and practical experimental results, showing a very good agreement. The theoretical results can be useful to minimize the complexity of the canceller with a controlled performance loss.

1. INTRODUCTION

The sense of hearing is extremely important for social participation, communication and personal safety. In a large number of cases, hearing aids are capable of compensating the deficiencies associated with hearing loss [1]. These devices are very complex systems compounded of a set of subsystems which interact with each other to improve intelligibility and provide better acoustical comfort to the user [2]. Due to their size and power consumption requirements, the availability of computational resources for each subsystem is strictly conditioned to the need of the others. As a result, each technique must be designed in the most sparingly way. One of the most important subsystems of a hearing aid is the feedback canceller. The feedback effect occurs due to the acoustic coupling between the loudspeaker and the microphone (due to their closeness) and can create a distortion in the signal supplied to the user. With the increasing gain of the device, this distortion is perceived as annoying whistling sounds, and there can be system instability. This problem is increased in wide-vent and open-fit equipments [2], due to the large opening in the ear-mould, which is needed to provide acoustic comfort to the user. Without the vent, there is the feeling of closed ear and the occlusion effect takes place [3]. The ventilation duct favours the acoustic feedback through the *feedback path*, shown as w^0 in Fig. 1. As a result, the maximum possible amplification (without perceived signal distortion or system instability) is reduced, often preventing from reaching the necessary amplification to compensate the hearing loss. To allow increased amplification, acoustical feedback cancellation algorithms are present in most state-of-the-art hearing aids. Although feedback cancellation is a

widely approached subject in the scientific literature, few papers have addressed the implementation issues related to these systems or have investigated its performance in real conditions where computational power is limited.

In this work, a promising feedback cancellation technique called “prediction error method” (originally proposed in [4]) was analysed for the practical case of interest in which the length of the adaptive filter is less than that of the feedback path. This condition is called “deficient length case” and occurs when the computational resources are limited by the available hardware or when this limitation is deliberately imposed by the designer, in order to save mathematical operations [5]. Under such a condition, using the approach described in [6], deterministic analytical equations were derived to predict the mean behaviour of the adaptive filters coefficients of the prediction error method technique. The predicted behaviour, obtained from the derived analytical equations, was compared with simulations and with results of controlled practical experiments, showing a very good agreement for different parameter settings. The obtained results allow the designer to reduce the feedback canceller computational cost with a controlled loss of performance.

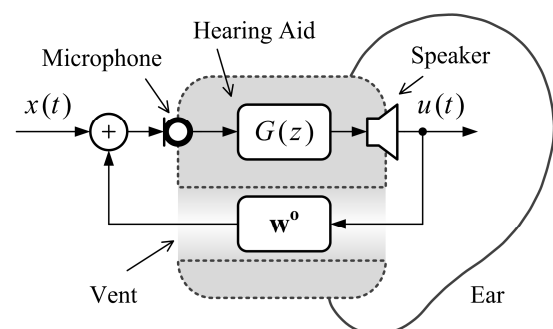


Figure 1 – Vent and acoustical feedback.

2. FEEDBACK CANCELLATION SCHEME

The feedback cancellation scheme is shown in Fig. 2, where n is the discrete time. The characteristics of amplification and group delay of the processing routines of the hearing aid are part of the called *direct path*. Without loss of generality, those are represented by the gain G and a delay of D samples (z^{-D}). In this work, in order to simplify the representation of the speech signals, the speech model considers only unvoiced

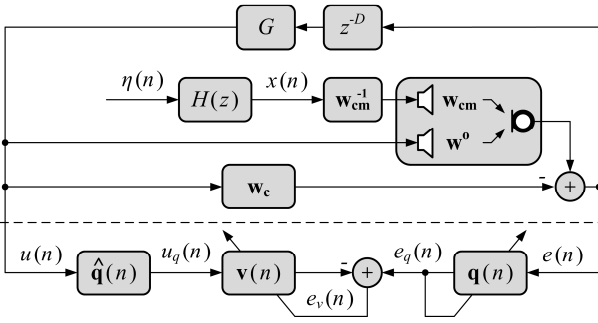


Figure 2 – Feedback cancellation scheme.

sounds. This limitation is a common practice in the analysis of the behaviour of hearing aids [6, 7, 8]. The speech signal $x(n)$ is modelled by an autoregressive (AR) process with transfer function $H(z)$ that contains the parameters of the vocal tract [9]. During the production of unvoiced sounds, the excitation $\eta(n)$ can be represented by a white Gaussian noise [10] with variance σ_η^2 . In general, during the occurrence of voiced sounds, the adaptation process is paralyzed. The feedback path consists of the speaker and microphone of the hearing aid, as well as the analog-to-digital, digital-to-analog converters, and the sound propagation environment. It is represented by the vector $\mathbf{w}^0 = [w_1^0 \ w_2^0 \ \dots \ w_N^0]^T$, which contains the N samples of the related impulse response. An initial estimate of \mathbf{w}^0 , which is calculated during the fitting process of the hearing aid, is stored in the vector \mathbf{w}_c . The cancelling filter $\mathbf{v}(n)$ contains the coefficients of the adaptive filter. After a previously defined number of iterations, ensuring a consistent estimate, the elements of $\mathbf{v}(n)$ are added to \mathbf{w}_c . $\mathbf{v}(n)$ is reset to a vector composed of zeros and the adaptation process restarts. Vector $\hat{\mathbf{q}}(n)$ is a copy of the prediction error filter $\mathbf{q}(n)$, which is responsible for obtaining the prediction error $e_q(n)$ [7]. The impulse responses \mathbf{w}_{cm} and \mathbf{w}_{cm}^{-1} are defined ahead, but ideally, their convolution should result in the unit sample function.

3. PREDICTION ERROR METHOD

The update equations for the cancelling filter $\mathbf{v}(n) = [v_1(n) \ v_2(n) \ \dots \ v_M(n)]^T$ and for the prediction error filter $\mathbf{q}(n) = [1 \ -\mathbf{p}(n)]^T$, are

$$\mathbf{v}(n+1) = \mathbf{v}(n) + \mu e_v(n) \mathbf{u}_q(n) \quad (1)$$

and

$$\mathbf{p}(n+1) = \mathbf{p}(n) + \rho e_q(n) \mathbf{e}(n-1) \quad (2)$$

where μ and ρ are the step sizes, $\mathbf{u}_q(n) = [u_q(n) \ u_q(n-1) \ \dots \ u_q(n-M+1)]^T$, $\mathbf{e}(n-1) = [e(n-1) \ e(n-2) \ \dots \ e(n-K)]^T$ and vectors $\mathbf{v}(n)$ and $\mathbf{p}(n)$ have lengths M and K , respectively.

4. THEORETICAL ANALYSIS

In this section, the theoretical models developed in [6] to predict the mean coefficients behaviour of the adaptive filters $\mathbf{v}(n)$ and $\mathbf{p}(n)$ are generalized for the case of deficient length [5]. To this end, the top of Fig. 2 (above the dashed line) is assumed stationary, i.e., \mathbf{w}_c is not updated.

Considering slow adaptation of $\mathbf{q}(n)$ [11],

$$e_v(n) = x_q(n) - \mathbf{u}_q^T(n) \mathbf{w}_c + \mathbf{u}_q^T(n) \mathbf{w}^0 - \mathbf{u}_q^T(n) \mathbf{v}(n) \quad (3)$$

where $x_q(n)$ represents the signal $x(n)$ filtered by $\mathbf{q}(n)$ and $\mathbf{u}_q(n) = [u_q(n) \ u_q(n-1) \ \dots \ u_q(n-N+1)]^T$. With \mathbf{w}_c stationary, the prediction error may be taken as

$$e_q(n) = \eta(n) - \mathbf{x}^T(n-1) \mathbf{h} - \mathbf{u}^T(n) \mathbf{v} - \mathbf{e}^T(n-1) \mathbf{p}(n) \quad (4)$$

where $\mathbf{x}(n-1) = [x(n-1) \ x(n-2) \ \dots \ x(n-L)]^T$ and $\mathbf{u}(n) = [u(n) \ u(n-1) \ \dots \ u(n-N+1)]^T$. The error vector $\mathbf{v} = [\mathbf{w}_c^T \ \mathbf{0}^T]^T - \mathbf{w}^0$ is given from the concatenation of vector \mathbf{w}_c , of dimension $(M \times 1)$, and the zero vector $\mathbf{0} = [0 \ 0 \ \dots \ 0]^T$, of dimension $(N-M \times 1)$, and the vector \mathbf{w}^0 for $M < N$. The coefficients of the AR process $H(z)$ are represented by the vector \mathbf{h} of size L . Taking the expected value of (1) and (2), after substitution of (3) and (4), respectively, we obtain:

$$\mathbb{E}\{\mathbf{v}(n+1)\} = [\mathbf{I} - \mu \mathbf{R}_{\mathbf{u}_q \mathbf{u}_q}] \mathbb{E}\{\mathbf{v}(n)\} - \mu [\mathbf{R}_{\mathbf{u}_q \mathbf{u}_q} \mathbf{v} - \mathbf{r}_{\mathbf{u}_q \mathbf{x}_q}] \quad (5)$$

and

$$\mathbb{E}\{\mathbf{p}(n+1)\} = [\mathbf{I} - \rho \mathbf{R}_{\mathbf{e} \mathbf{e}}] \mathbb{E}\{\mathbf{p}(n)\} - \rho [\mathbf{R}_{\mathbf{e} \mathbf{u}} \mathbf{v} + \mathbf{R}_{\mathbf{e} \mathbf{x}} \mathbf{h}] \quad (6)$$

where it was assumed independence between $\mathbf{u}_q(n) \mathbf{u}_q^T(n)$ and $\mathbf{v}(n)$, as well as between $\mathbf{e}(n) \mathbf{e}^T(n-1)$ and $\mathbf{p}(n)$ [12]. Also

$$\begin{cases} \mathbf{R}_{\mathbf{u}_q \mathbf{u}_q} = \mathbb{E}\{\mathbf{u}_q(n) \mathbf{u}_q^T(n)\} & \mathbf{R}_{\mathbf{e} \mathbf{e}} = \mathbb{E}\{\mathbf{e}(n-1) \mathbf{e}^T(n-1)\} \\ \mathbf{R}_{\mathbf{u}_q \mathbf{u}_q} = \mathbb{E}\{\mathbf{u}_q(n) \mathbf{u}_q^T(n)\} & \mathbf{R}_{\mathbf{e} \mathbf{u}} = \mathbb{E}\{\mathbf{e}(n-1) \mathbf{u}_q^T(n)\} \\ \mathbf{r}_{\mathbf{u}_q \mathbf{x}_q} = \mathbb{E}\{\mathbf{u}_q(n) x_q(n)\} & \mathbf{R}_{\mathbf{e} \mathbf{x}} = \mathbb{E}\{\mathbf{e}(n-1) \mathbf{x}^T(n-1)\} \end{cases} \quad (7)$$

The matrix $\mathbf{R}_{\mathbf{u}_q \mathbf{u}_q}$ is given by the first M columns of the matrix $\mathbf{R}_{\mathbf{u}_q \mathbf{u}_q}$, whose elements are defined by [6]:

$$R_{u_q u_q(i,j)} = G^2 \sum_{k=1}^{K+1} \sum_{l=1}^{K+1} \mathbb{E}\{q_k(n)\} \mathbb{E}\{q_l(n)\} r_{ee}(l+j-i-k) \quad (8)$$

($i=1,2,\dots,M$; $j=1,2,\dots,N$)

where $q_k(n)$ and $q_l(n)$ are elements of $\mathbf{q}(n)$. The remaining elements of (5) and (6) are

$$r_{u_q x_q(i)} = G \sum_{k=1}^{K+1} \sum_{l=1}^{K+1} \mathbb{E}\{q_k(n)\} \mathbb{E}\{q_l(n)\} r_{xe}(l+i-k-1+D) \quad (9)$$

($i=1,2,\dots,M$)

$$R_{ee(i,j)} = r_{ee}(i-j) \quad \begin{cases} i=1,2,\dots,K \\ j=1,2,\dots,K \end{cases} \quad (10)$$

$$R_{eu(i,j)} = G r_{ee}(i-j-D+1) \quad \begin{cases} i=1,2,\dots,K \\ j=1,2,\dots,N \end{cases} \quad (11)$$

$$R_{ex(i,j)} = r_{xe}(i-j) \quad \begin{cases} i=1,2,\dots,K \\ j=1,2,\dots,L \end{cases} \quad (12)$$

where $r_{ab}(l) = \mathbb{E}\{a(n)b(n-l)\}$ is the correlation between the generic random variables $a(n)$ and $b(n)$. Following the calculations described in [8]:

$$r_{ee}(l) = r_{xe}(l) - G \mathbf{r}_{ee}^T(l-D) \mathbf{v} \quad (13)$$

and

$$r_{xe}(l) = \sum_{k=1}^L \frac{\sigma_\eta^2 (-a_k)^{l-1+L} [1 + G(-a_k)^D \Psi(-a_k) \mathbf{v}]^{-1}}{\prod_{i=1, i \neq k}^L (a_i - a_k) \prod_{i=1}^L (1 - a_i a_k)} \quad (14)$$

for $l \geq 1-L$, $\mathbf{r}_{ee}(l-D) = [r_{ee}(l-D) \ r_{ee}(l-D-1) \ \dots \ r_{ee}(l-D-N+1)]^T$, $\Psi(-a_k) = [1 \ -a_k^{-1} \ -a_k^{-2} \ \dots \ -a_k^{-N+1}]^T$ and the coefficients $-a_k$ are poles of $H(z)$.

4.1 Steady-State Conditions

In steady-state, assuming convergence of the coefficients, equations (5) and (6) result in:

$$\lim_{n \rightarrow \infty} E\{v(n)\} = -R_{uquq}^{-1} R_{uquq} v + R_{uquq}^{-1} r_{uqxq} \quad (15)$$

and

$$\lim_{n \rightarrow \infty} E\{p(n)\} = -R_{ee}^{-1} R_{eu} v - R_{ee}^{-1} R_{ex} h \quad (16)$$

In the case of sufficient length, $v(n)$ converges to the non-cancelled part of w^0 (difference between w^0 and w_c), in addition to a bias term $R_{uquq}^{-1} r_{uqxq}$. This term is function of $x_q(n)$ and can be reduced by the filtering process realized by $q(n)$. Equations (15) and (16) generalizes the results presented in [6] for the deficient case.

5. EXPERIMENTAL SETUP

The acoustic chamber built for the practical experiments is shown in Fig. 3 and consists of a Medium Density Fibre-board box with dimensions $100 \times 70 \times 70 \text{ cm}^3$, internally covered with 5 cm of acoustic insulation foam. It contains a loudspeaker (Edifier R1000TCN), a mobile screen and a conventional mannequin with a silicone ear and acoustic canal. A Behind-The-Ear digital hearing aid (Voyager GN Resound) was positioned with the speaker attached to the ear-mould through a plastic tube. The ear-mould has a vent of 1 mm in diameter. The microphone and speaker of the hearing aid were connected to the Voyageur Dedicated Development Platform (Sound Design Technologies), which is based on the GA3280 [13] hybrid circuit ($5.46 \times 3.15 \times 1.70 \text{ mm}^3$). The sampling frequency was 15.625 kHz and the audio samples were quantized with 20 bits.

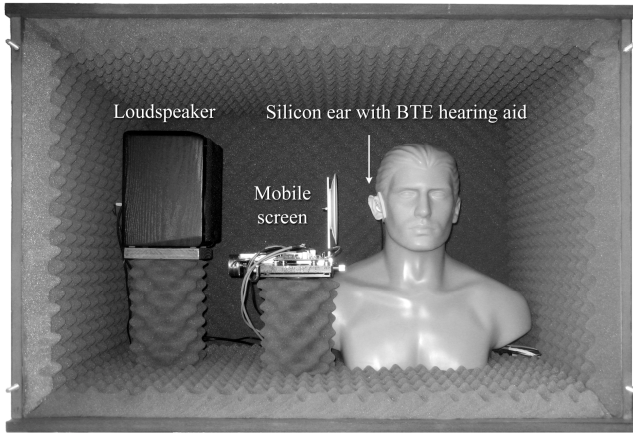


Figure 3 – Internal view of the acoustic chamber.

In the experiments, digitally recorded sounds were reproduced by a secondary loudspeaker to provide repeatability. Nevertheless, it was verified that the effects of the loudspeaker, sound propagation environment and microphone (impulse response w_{cm} in Fig. 2) changed the statistical properties of the desired speech signal. Thus, a fixed compensation filter with impulse response w_{cm}^{-1} was used to equalize the undesired effects and permit fair comparisons between analytical results and practical experiments. However, ob-

taining the transfer function $W_{cm}^{-1}(z)$ of w_{cm}^{-1} by inverting the transfer function $W_{cm}(z)$ of w_{cm} is not possible due to the latter being non-minimum phase. A stable solution that provides a close approximation to the unstable transfer function $W_{cm}^{-1}(z)$ was achieved through *adaptive inverse modelling* [14].

5.1 System Configuration

The feedback path impulse response w^0 , identified in the acoustic chamber, is shown in Fig. 4. It was used to obtain theoretical predictions by equations (5) and (6). The vector w_c was initialized with zeros and was not updated. It was experimentally verified that distortions caused by w_{cm} were adequately compensated by the fixed compensation filter w_{cm}^{-1} . The input signal was a simulated unvoiced utterance modelled by a 21 order autoregressive model $H(z)$, estimated by the Burg method [15], obtained from a 20 milliseconds male speaker epoch of the /s/ phoneme. The coefficients of the AR process $H(z)$ contained in vector h are shown in Fig. 5. The variance σ_η^2 was empirically defined so that the variance of the speech signal $x(n)$ corresponded to 60 dB SPL (sound level of a normal conversation).

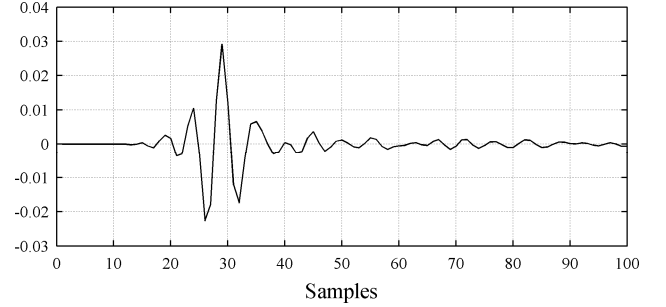


Figure 4 – Impulse response w^0 .

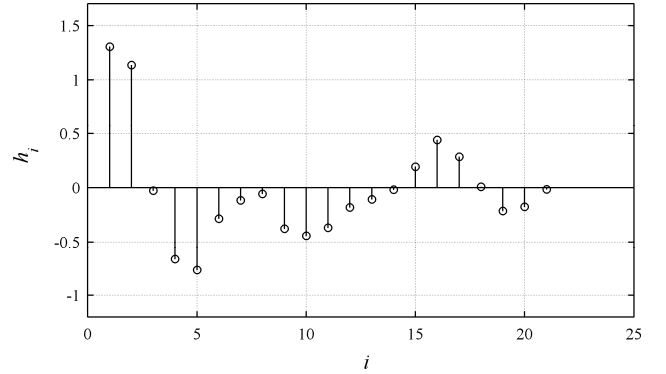


Figure 5 – Coefficients of the AR process $H(z)$.

6. RESULTS

In this section, the theoretical performance of the prediction error method, given by equations (5) and (6), is compared with Monte Carlo simulations [16] and practical experiments for different lengths of $v(n)$ and $p(n)$ as shown in Table 1. For each setup, 10 realizations were made each one with $2 \cdot 10^6$ iterations. Due to practical limitations of the Voyageur platform, the coefficients were extracted with a decimation factor of 2000. The same procedure was performed on the theoreti-

Table 1 – Algorithm parameters.

Parameter	Symbol	Value
Direct path gain	G	6
Direct path delay	D	78
Step size of $\mathbf{v}(n)$	μ	0.02
Step size of $\mathbf{q}(n)$	ρ	32
Length of $\mathbf{v}(n)$	M	25, 26 and 50
Length of $\mathbf{p}(n)$	K	3, 7, 9 and 21

cal results and simulations to enable comparison. The experiments were carried out with small step sizes in order to support the considerations used on the derivation of the theoretical model. The direct path delay is known to reduce the bias term $\mathbf{R}_{uquq}^{-1} \mathbf{r}_{uqxq}$ [8], however it should be kept under 6 ms to avoid user discomfort [17]. The chosen value of D corresponds to 5ms for the sampling frequency used.

6.1 Coefficients Evolution

Figs. 6 to 8 illustrate the mean coefficients behaviour of $v_{21}(n)$, $v_{22}(n)$ and $v_{24}(n)$, respectively, for different lengths of the cancelling filter $\mathbf{v}(n)$.

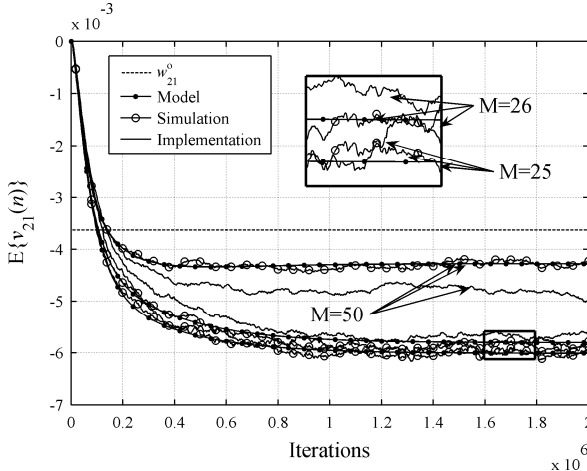


Figure 6 – Mean evolution of the coefficient $v_{21}(n)$ for $K=21$.

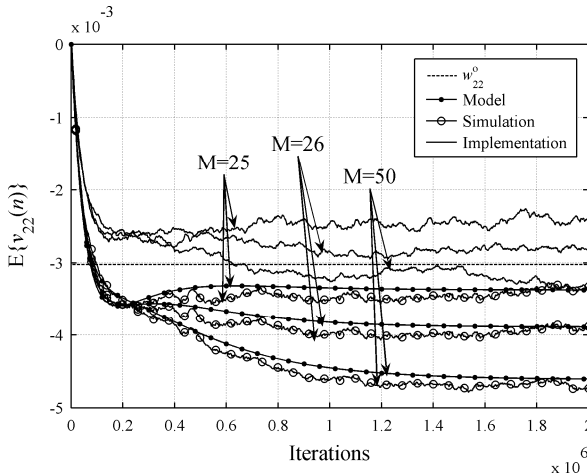


Figure 7 – Mean evolution of the coefficient $v_{22}(n)$ for $K=21$.

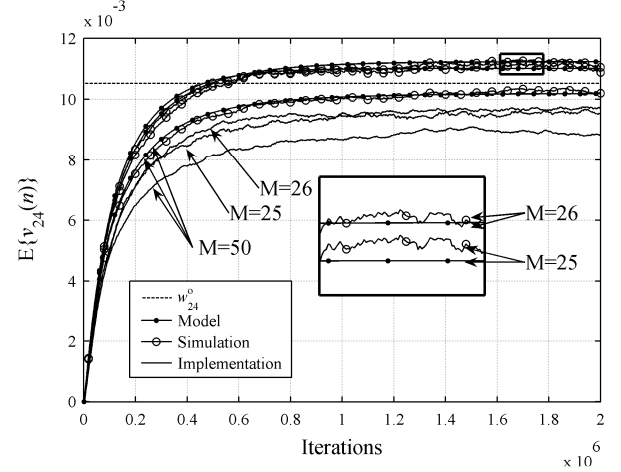


Figure 8 – Mean evolution of the coefficient $v_{24}(n)$ for $K=21$.

The optimal values for each coefficient shown, corresponding to the samples of the feedback path \mathbf{w}^0 , are illustrated by a dotted horizontal straight line. In Figs. 6 and 8, a zoomed inset has been added to allow a better distinction among the curves in steady-state conditions.

6.2 Misadjustment of the Coefficients

In Figs. 9 and 10, the misadjustment of the coefficients, defined as

$$\zeta(\mathbf{v}(n), \mathbf{v}) = \frac{\|E\{\mathbf{v}^T(n) \mathbf{0}^T\} - [-\mathbf{v}]\|_2^2}{\|\mathbf{v}\|_2^2}, \quad (17)$$

provides an overview of the general behaviour of $\mathbf{v}(n)$. In (17) the symbol $\|\cdot\|_2$ represents the Euclidean norm. In Fig. 9, the length K of $\mathbf{p}(n)$ is kept fixed, while the length M of $\mathbf{v}(n)$ is kept fixed in Fig. 10. In both cases, the misadjustment is presented in a dB scale.

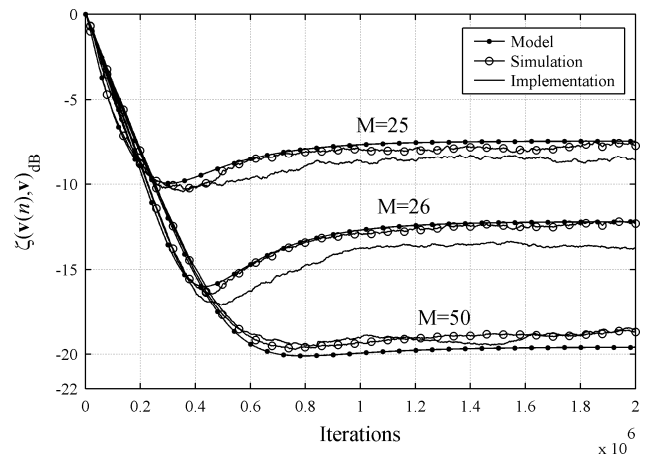


Figure 9 – Misadjustment of $\mathbf{v}(n)$ for $K=21$.

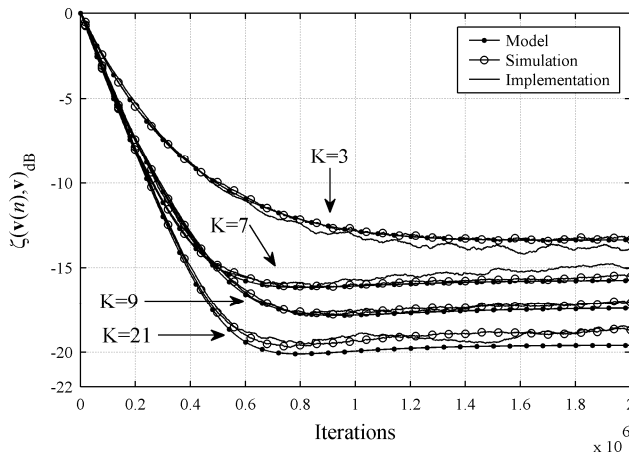


Figure 10 – Misadjustment of $\mathbf{v}(n)$ for $M=50$.

7. DISCUSSION

As predicted by equation (15), the bias prevents the adaptive coefficients to reach the optimum values in steady-state. In Figs. 6 and 8, the experimental results tend to follow the model predictions and simulations results, regardless the closeness to the optimum values. In Fig. 7, the theoretical model and simulation results are below the optimal value while the experimental results are concentrated above it. However, in each case, the proportion between the curves remains for different values of M . Despite differences in the evolution of some individual coefficients, the misadjustment of the coefficients (Figs. 9 and 10) indicates a global excellent agreement between model, simulation and practical experiments. In Figs. 9 and 10, it is observed that the model is slightly conservative, since the practical results are in general slightly better than the theoretically expected. In Fig. 9, the vector $[\mathbf{v}^T(n) \mathbf{0}^T]^T$ approaches \mathbf{w}^0 in steady-state, with increasing M . The same happens in Fig. 10 with the increasing length of the predictor. Also in Fig. 10, it is shown that the use of the predictor accelerates the convergence of the cancelling filter $\mathbf{v}(n)$ and minimizes the bias. The presented speech production model considered only unvoiced sounds.

8. CONCLUSION

This work presented an analytical model for the mean coefficients behaviour of the deficient length LMS algorithm, associated with the prediction error method for feedback cancellation in hearing aids. Statistical simulations and practical experiments using a dedicated signal processor confirm the validity of the results. The derived equations can be used to design the canceller with a minimum complexity for a desired performance.

9. ACKNOWLEDGMENTS

The authors wish to thank to Acústica Amplivox company for logistical support. This work was supported by the Brazilian Ministry of Science and Technology (CNPq) under grants 559418/2008-6, and 303803/2009-6.

REFERENCES

- [1] H. Dillon, *Hearing aids*. Boomerang press, 2001.
- [2] K. Chung, "Challenges and recent developments in hearing aids - Part II. Feedback and occlusion effect reduction strategies, Laser shell manufacturing processes, and other signal processing technologies," *Trends in Amplification*, vol. 8, no. 4, pp. 125-164, 2004.
- [3] J. Mejia, H. Dillon, and M. Fisher, "Active cancellation of occlusion: an electronic vent for hearing aids and hearing protectors," *Journal of the Acoustical Society of America*, vol. 124, no. 1, pp. 235-240, 2008.
- [4] L. Ljung, *System Identification: Theory for the User*, Prentice Hall, 1987.
- [5] K. Mayyas, "Performance analysis of the deficient length LMS adaptive algorithm," *IEEE Transactions on Signal Processing*, vol. 53, no. 8, pp. 2727-2734, 2005.
- [6] Y. Montenegro, J.C.M. Bermudez, "Mean weight behaviour of coupled LMS adaptive systems applied to acoustic feedback cancellation in hearing aids," *Lecture Notes in Computer Science*, vol. 5099, pp. 527-535, 2008.
- [7] A. Spriet, I. Proudler, M. Moonen, J. Wouters, "Adaptive feedback cancellation in hearing aids with linear prediction of the desired signal," *IEEE Transactions on Signal Processing*, vol. 53, no. 10, pp. 3749-3763, 2005.
- [8] M. Siqueira, A. Alwan, "Steady-state analysis of continuous adaptation in acoustic feedback reduction systems for hearing-aids," *IEEE Transactions on Speech and Audio Processing*, vol. 8, no. 4, pp. 443-453, 2000.
- [9] P.C. Loizou, *Speech enhancement: theory and practice*, CRC, 2007.
- [10] J.R. Deller Jr, J.G. Proakis, J.H. Hansen, *Discrete Time Processing of Speech Signals*, Prentice Hall PTR Upper Saddle River, NJ, USA, 1993.
- [11] M. Mboup, M. Bonnet, N. Bershad, "LMS coupled adaptive prediction and system identification: a statistical model and transient mean analysis," *IEEE Transactions on Signal Processing*, vol. 42, no. 10, pp. 2607-2615, 1994.
- [12] J. Minkoff, "Comment on the unnecessary assumption of statistical independence between reference signal and filter weights in feedforward adaptive systems," *IEEE Transactions on Signal Processing*, vol. 49, no. 5, pp. 1109, 2001.
- [13] GA3280, "Voyager open platform dsp system for ultra low power audio processing," Gennum, pp. 1-17, 2006.
- [14] B. Widrow, E. Walach, *Adaptive Inverse Control*, Prentice Hall PTR Upper Saddle River, NJ, USA, 1996.
- [15] J.P. Burg, "A new analysis technique for time series data," in *NATO Advanced Study Institute on Signal Processing*, Enschede, Netherlands, Aug. 1968.
- [16] S. Raychaudhuri, "Introduction to Monte Carlo Simulation," in *Proc. of the 40th Winter Simulation Conference*, Miami, Florida, 2008, pp. 91-100.
- [17] M. A. Stone, B. C. J. Moore, K. Meisenbacher, R. P. Derleth, "Tolerable Hearing Aid Delays. V. Estimation of Limits for Open Canal Fittings," *Ear & Hearing*, vol. 29, no. 4, pp. 601-617, 2008.